

A detailed study of the 5 Hz quasi-periodic oscillations in the bright X-ray transient and black-hole candidate GRS 1739–278

Rudy Wijnands^{1*}, Mariano Méndez², Jon M. Miller¹, Jeroen Homan³

¹ Center for Space Research, Massachusetts Institute of Technology, 77 Massachusetts Avenue, Cambridge, MA 02139-4307, USA

² SRON Laboratory for Space Research, Sorbonnelaan 2, NL-3584 CA, Utrecht, The Netherlands

³ Astronomical Institute “Anton Pannekoek”, University of Amsterdam, Kruislaan 403, NL-1098 SJ Amsterdam, The Netherlands

1 December 2018

ABSTRACT

We present a detailed study of the 5 Hz quasi-periodic oscillation (QPO) recently discovered in the bright X-ray transient and black-hole candidate GRS 1739–278 (Borozdin & Trudolyubov 2000) during a *Rossi X-ray Timing Explorer* observation taken on 1996 March 31. In total 6.6 ksec of on-source data were obtained, divided in two data sets of 3.4 and 3.2 ksec which were separated by ~ 2.6 ksec. The 5 Hz QPO was only present during the second data set. The QPO increased in strength from below 2% rms amplitude for photon energies below 4 keV to $\sim 5\%$ rms amplitude for energies above 10 keV. The soft QPO photons (below 5 keV) lagged the hard ones (above 10 keV) by almost 1.5 radian. Besides the QPO fundamental, its first overtone was detected. The strength of the overtone increased with photon energy (from $< 2\%$ rms below 5 keV to $\sim 8\%$ rms above 10 keV). Although the limited statistics did not allow for an accurate determination of the lags of the first overtone, indications are that also for this QPO the soft photons lagged the hard ones. When the 5 Hz QPO was not detected (i.e., during the first part of the observation), a broad noise component was found for photon energies below 10 keV but it became almost a true QPO (with a Q value of ~ 1.9) above that energy, with a frequency of ~ 3 Hz. Its hard photons preceded the soft ones in a way reminiscent of the 5 Hz QPO, strongly suggesting that both features are physically related. We discuss our finding in the frame work of low-frequency QPOs and their properties in BHCs.

Key words: accretion, accretion discs – stars: black-hole – stars: individual: GRS 1739–278 – X-rays: stars

1 INTRODUCTION

Before the launch of the *Rossi X-ray Timing Explorer* (*RXTE*), the usual picture for black-hole candidates (BHCs) was simple and one-dimensional: the changes in the X-ray spectra and the rapid X-ray variability are caused by changes in the mass accretion rate \dot{M} (Tanaka & Lewin 1995; van der Klis 1995). In the BHC low-state (LS), \dot{M} is low and the spectra are hard. The LS power spectra are dominated by a very strong (20%–50% rms amplitude) band-limited noise which follows approximately a power-law with index 1 at high frequencies, but below a certain frequency (the break frequency) the power spectrum becomes roughly flat. Above this frequency a broad bump or a quasi-periodic oscillation (QPO) is often present, although also QPOs with

similar frequencies as the break frequency are observed. In some sources, a second break is visible in the power spectrum, above which the power-law index increases to about ~ 2 . In the high state (HS), \dot{M} is higher, the spectra are much softer, and in the power spectra only a weak (a few percent) power-law noise component is present. In the very high state (VHS), \dot{M} is the highest, the spectra are harder but not as hard as in the LS, and in the power spectra, noise is present similar to either the weak HS noise or the LS band-limited noise (although only with a strength of 1%–15% rms). QPOs near 6 Hz are detected sometimes with a complex harmonic structure.

With the many observations performed with *RXTE* on BHCs, the behaviour of BHCs turned out to be much more complex than previously thought. First of all, *RXTE* has expanded the range of frequencies at which the BHCs show variability up to 450 Hz (e.g., Remillard et al. 1999a,b; Cui

* Chandra Fellow; Email: rudy@space.mit.edu

et al. 2000; Homan et al. 2001; Strohmayer 2001). The nature of these BHC high-frequency QPOs is unclear, although it has been suggested that they might be related to the twin kHz QPOs in the neutron star systems (Psaltis et al. 1999). Also, with *RXTE* in many BHCs the VHS has now been detected and the associate low-frequency (<20 Hz) QPOs have been found (e.g., Remillard et al. 1999b; Borozdin & Trudolyubov 2000; Revnivtsev, Trudolyubov, & Borozdin 2000; Dieters et al. 2000; Cui et al. 2000; Homan et al. 2001), indicating that these QPOs are a common feature of BHCs. The phenomenology of these QPOs is very complex and they are observed during different luminosity levels (at levels significantly below the highest observed luminosities, i.e., not only during the VHS but at states intermediate between the LS and the HS; e.g., Homan et al. 2001). The phenomenology of these QPOs is such that even in individual sources, the QPO interrelationships are not fully understood (see, e.g., Wijnands et al. 1999 or Homan et al. 2001). The relationship between the QPOs observed in different BHCs is even less well understood. However, from a detailed study of the state behaviour in XTE J1550–564 it is clear that the one-dimensional picture described above for the BHC states (depending only on \dot{M}) does not hold in this particular source and another extra parameter is needed to explain its behaviour (Homan et al. 2001). Similar behaviour might also be observable for the other BHCs, however, not much information about this is presently available.

One of the most recent additions to the collection of BHCs which exhibit QPOs near 6 Hz is the X-ray transient and BHC GRS 1739–278. At the end of March 1996, this new X-ray transient was discovered with the SIGMA telescope on board *Granat* (Paul et al. 1996; Vargas et al. 1997). Soon after the discovery of this new X-ray source its radio and optical counterpart were discovered (Hjellming et al. 1996; Mirabel et al. 1996; Marti et al. 1997). From a *ROSAT* observation of the source an extinction of $A_v = 14 \pm 2$ was derived, implying that the source is located at a distance of 6–8.5 kpc and that it was radiating at least near the Eddington limit for a $1 M_\odot$ compact object (Dennerl & Greiner 1996; Greiner, Dennerl, & Predehl 1996). In X-rays, GRS 1739–278 was studied by the TTM experiment on board *Mir-Kvant* and by the PCA instrument on board *RXTE* (Borozdin, Alexandrovich, & Sunyaev 1996; Takeshima et al. 1996; Borozdin et al. 1998). The *RXTE* data showed that on 1996 March 31, the source was in the canonical black-hole very high state and the *RXTE* observations taken in 1996 May showed that the source had transit to the canonical high state. Recently, Borozdin & Trudolyubov (2000) reported the discovery of a 5 Hz QPO during the 1996 March 31 *RXTE* observation. Because the QPO behaviour of BHCs is not well understood, we decided to study the properties of this 5 Hz QPO in GRS 1739–278 in more detail (e.g., time variability, phase lags).

2 OBSERVATION AND ANALYSIS

RXTE observed GRS 1739–278 on several occasions during its 1996 outburst. For a detailed overview of the *RXTE* observations, we refer to Borozdin et al. (1998). In this paper, we concentrate on the 1996 March 31 observation during which the 5 Hz QPO was discovered (Borozdin & Tru-

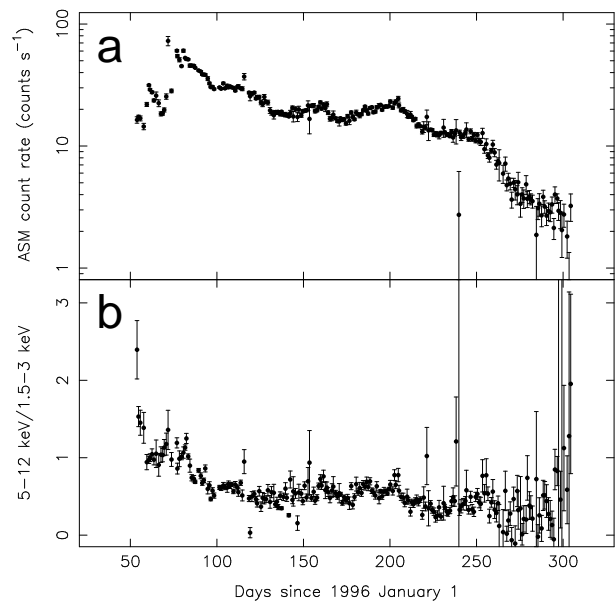


Figure 1. The daily-averaged *RXTE*/ASM light curve of GRS 1739–278 (a) and the 5–12 keV/1.5–3 keV count rate ratio curve of the source (b). The 5 Hz QPO was detected on 1996 March 31 which is day 90 in this figure.

dolyubov 2000). In order to avoid confusion with the bright neutron-star X-ray transient GRO J1744–28, the satellite was not pointed directly at GRS 1739–278 but had an off-site pointing of ~ 11 arcmin (see Takeshima et al. 1996, Borozdin et al. 1998). Borozdin & Trudolyubov (2000) showed that the QPO almost certainly originated from GRS 1739–278 and not from GRO J1744–28.

During the 1996 March 31 observation, data were simultaneously collected in the Standard2f mode (129 photon energy channels with 16 s time resolution), in the single bit modes SB_125US_0_13_1S and SB_125US_14_35_1S (1 photon energy channel, 128 μ s time resolution), in the binned mode B_2MS_16A_0_35_Q (16 photon energy channels, 2 ms time resolution), and in the event mode E_16US_64M_36_1S (64 photon energy channel, 16 μ s time resolution). We used the Standard2f data to create a light curve and the colours. For this analysis, we only used the data during which all 5 detectors were on; because of this restriction, we disregarded the first ~ 1000 seconds of the observation during which 2 out of the 5 detectors were off. For the analysis of the rapid X-ray variability we used all data available, unless otherwise noted. The high time resolution modes (single bit, binned, and event mode data) were used to calculate discrete Fourier transforms between 1/16–4096 Hz or 1/16–256 Hz, from which the power and cross spectra were calculated. The power spectra were fitted with a constant (representing the dead-time modified Poisson noise), a power-law (for the low-frequency noise component), and one or more Lorentzians (for the peaked noise component and the QPOs). The uncertainties in the fit parameters were calculated using $\Delta\chi^2 = 1$ and upper limits using $\Delta\chi^2 = 2.7$ which yields 95% confidence levels. The phase lags of the QPOs were calculated for a frequency interval equal to the FWHM of the Lorentzians used to fit the QPOs, centred on the peak frequency of these Lorentzians. To correct for the small dead-time effects on the

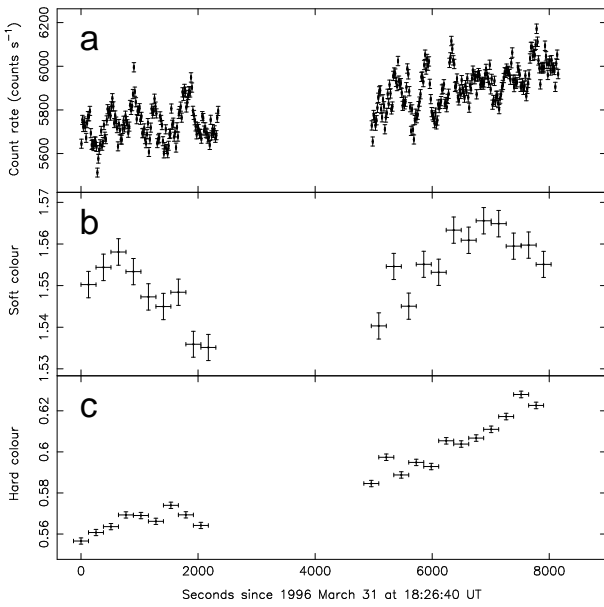


Figure 2. The 2–60 keV light curve (a), the soft colour (b), and the hard colour (c) of GRS 1739-278 on 1996 March 31. The first ~ 1000 seconds of the observation were not used because only 3 out of the 5 detectors were on. The soft colour is the 3.7–6.2 keV/2.2–3.7 keV count rate ratio and hard colour the 6.2–16.2 keV/2.2–3.7 keV count rate ratio. The time resolution of the light curve is 16 seconds in order to show the rapid count rate variations. The time resolution of the colours is 256 seconds in order to decrease the errors on the colours. The count rates were corrected for background and off-set (the collimator correction factor was 1.1572) but not for dead-time ($\sim 15\%$). The gap in the data is due to an Earth occultation of the source and a passages of the satellite through the SAA.

phase lags, we subtracted the average 50–125 Hz cross vector from the cross spectra (see van der Klis et al. 1987). The single bit and the event mode data were used to search for high frequency (>100 Hz) QPOs.

3 RESULTS

3.1 Light curve and colours

The *RXTE* all sky monitor (ASM[†]) light curve (1.5–12 keV) of the source is shown in Figure 1a (see also Borozdin et al. 1998; Borozdin & Trudolyubov 2000). The outburst light curve of GRS 1739-278 can be classified as a typical fast rise, exponential decay light curve, although with multiple maxima in the decay. At the peak of the outburst the flux was about 1 Crab, which makes this source a bright X-ray transient. The 5–12 keV/1.5–3 keV count rate ratio curve is shown in Figure 1b, which shows that the spectrum was hardest at the start of the outbursts (during the rise, before the peak of the outburst) and gradually became softer. The 5 Hz QPO was discovered during the 1996 March 31 *RXTE*

[†] The quick-look ASM data used in this paper can be obtained from http://xte.mit.edu/ASM_lc.html and are provided by the ASM/*RXTE* team. See Levine et al. (1996) for a detailed description of the ASM.

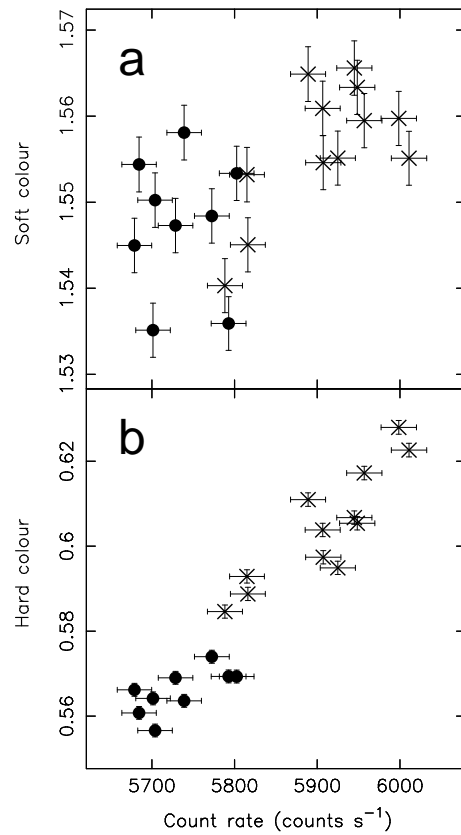


Figure 3. Hardness-intensity diagrams (HIDs) of GRS 1739-278 on 1996 March 31: (a) the ‘soft’ HID and (b) the ‘hard’ HID. The first ~ 1000 seconds of the observation were not used because only 3 out of the 5 detectors were on. The soft colour is the 3.7–6.2 keV/2.2–3.7 keV count rate ratio and hard colour the 6.2–16.2 keV/2.2–3.7 keV count rate ratio. The count rate was measured in the 2–60 keV energy range and was corrected for the satellite off-set of ~ 11 arcmin. The time resolution is 256 seconds. The count rates were corrected for background but not for dead-time. The solid dots are the data for the first part of the observation; the crosses for the second part.

observation, which is day 90 in this figure, at a time when the source was already considerable weaker than at the peak of the outburst, and the X-ray spectrum had significantly softened compared to previous days.

The 2–60 keV light curve of the *RXTE*/PCA observation of 1996 March 31 is shown in Figure 2a. The gap between the two parts of the light curve is due to an Earth occultation of the source and a passage of the satellite trough the South Atlantic Anomaly (SAA). The light curve has been corrected for the instrument off-set (the collimator correction factor was 1.1572). In Figure 2b and c, the soft and the hard colour curves are shown, respectively. As soft colour we used the 3.7–6.2 keV/2.2–3.7 keV count rate ratio and as hard colour we used the 6.2–16.2 keV/2.2–3.7 keV count rate ratio.

From Figure 2a, it is apparent that the source was highly variable on time scales of minutes. Also, it can be observed that, although the source count rate was gradually decreasing on time scales of weeks, the count rate increased with time during this observation, which is most clearly visible in the second part of the observation. The soft colour

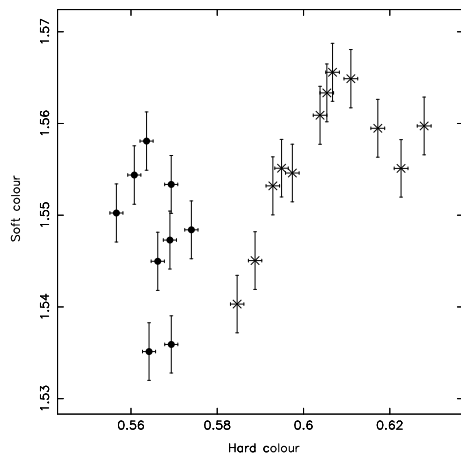


Figure 4. Colour-colour diagram of GRS 1739-278 on 1996 March 31. The first ~ 1000 seconds of the observation were not used because only 3 out of the 5 detectors were on. The soft colour is the 3.7–6.2 keV/2.2–3.7 keV count rate ratio and hard colour the 6.2–16.2 keV/2.2–3.7 keV count rate ratio. The time resolution is 256 seconds. The data were corrected for back-ground. The solid dots correspond to the first part of the observation; the crosses to the second part.

(Fig. 2*b*) did not show a clear correlation with time, whereas the hard colour (Fig. 2*c*) clearly increased with time (best visible in the second part of the observation). Because the count rate also increased with time (Fig. 2*a*), in the ‘hard’ hardness-intensity diagram (HID; as colour the hard colour was used; Fig. 3*b*), the hard colour showed a clear positive correlation with the count rate, but in the ‘soft’ HID (as colour the soft colour was used; Fig. 3*a*), the soft colour did not show such a good correlation (as expected from the lack of a good correlation of the soft colour with time), although also the soft colour seemed to slightly increase with count rate. This is reflected in the colour-colour diagram (CD; Fig. 4) which shows that the soft colour tended to increase when also the hard colour increased.

3.2 Rapid X-ray variability

In order to study the rapid X-ray variability (i.e., the 5 Hz QPO discovered by Borozdin & Trudolyubov 2000), we first produced a dynamical power spectrum of the data (Fig. 5). From this figure, it is apparent that the QPO was only clearly present in the second part of the data and not in the first part. To check this, we created a power spectrum for each part separately (shown in Figures 6*a* and *b*). Using the energy range 2.8–31.7 keV, a very significant 5 Hz QPO (rms amplitude $2.33\% \pm 0.07\%$ [$\sim 18\sigma$]; frequency 5.09 ± 0.03 Hz, width 1.11 ± 0.09 Hz) and its first overtone (rms amplitude 1.9 ± 0.1 [$\sim 9\sigma$]; frequency 10.2 ± 0.2 Hz; width 2.7 ± 0.4 Hz) were present during the second part of the observation, but during the first part the 5 Hz QPO was not present (but see below), although a weak noise component around a few hertz was (see Fig. 6). During the second part, an extra noise component at low frequencies was also present which was fitted with a power-law (rms amplitude $1.16\% \pm 0.09\%$ and with a power-law index of 0.71 ± 0.08).

To study the energy dependence of the rapid X-ray vari-

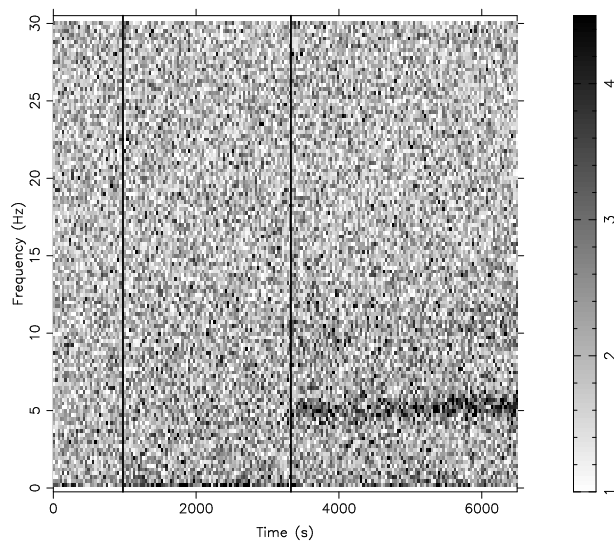


Figure 5. Dynamical power spectrum of the whole observation, including the part where only 3 detectors were on. The time resolution of the data is 32 seconds. The first black line indicates when the number of detectors that were on changed from 3 to 5. The second black line indicates the gap between the two data parts due to Earth occultation of the source and a passage of the satellite trough the SAA (~ 2600 seconds).

ability, we made power spectra of each part in a soft band (2–8.7 keV; Figs. 6*c* and *d*) and a hard one (8.7–60 keV; Figs. 6*e* and *f*). At first glance, the noise component in the first part of the observation did not show any clear dependence on energy (but see below), but the QPOs in the second part did: at low energies the fundamental was stronger than its overtone, but at higher energies they were of comparable strength. The exact dependence of the QPO amplitude on photon energy is shown in Figure 7*a* for the fundamental and in Figure 7*b* for the first overtone (see also Tab. 1). From these figures, it is clear that at the highest energies (> 10 keV) the overtone was even stronger than the fundamental, demonstrating that the overtone had a steeper dependence on photon energy than the fundamental.

To study the behaviour of the QPO fundamental in the second part with count rate and colours, we used 256 s data segments to track the QPO parameters in time. The results are shown in Figure 8. The frequency of the QPO increased slightly when the count rate increased (Fig. 8*a*) but more strongly when the hard colour increased (Fig. 8*b*), suggesting that the hard colour is a better tracer of the QPO frequency than the count rate. The other parameters of the QPO (rms amplitude and FWHM) did not show clear correlations either with the count rate or the colours.

We calculated cross spectra in order to study the phase lags of the QPOs. The phase lags between two broad energy bands as a function of frequency is shown in Figures 6*g* and *h*. Clearly the 5 Hz QPO had negative phase lags (Fig. 6*h*), meaning that the hard photons of the 5 Hz QPO preceded the soft ones. The phase lags of the 5 Hz QPO as a function of photon energy are shown in Figure 7*c*. The lags increased with increasing photon energy. The lowest energy bin is not shown because the QPO was not detected in this energy band. Using two broad energy bands, we find a $\sim 3\sigma$

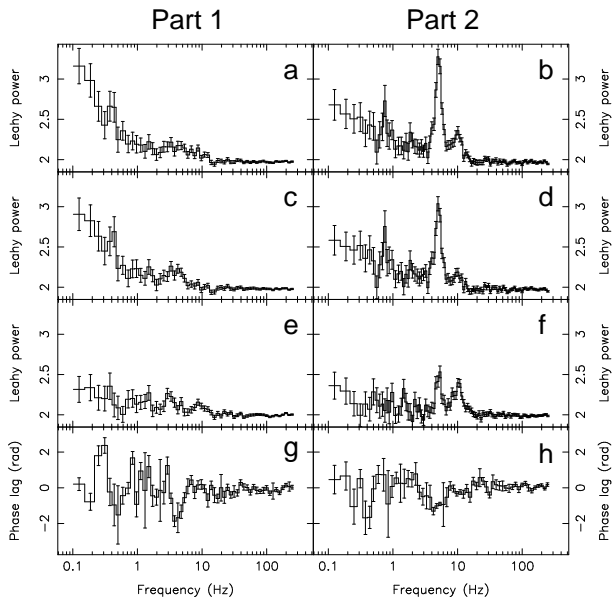


Figure 6. Leahy normalized (Leahy et al. 1983) power spectra of the first (*a*, *c*, and *e*) and second (*b*, *d*, and *e*) part of the observation in the energy range of 2–60, 2–8.7, and 8.7–60 keV, respectively. The Poisson level has been not subtracted. Cross spectra of the first (*g*) and second (*h*) part of the observation, calculated between 2.8–8.7 and 8.7–60 keV. Negative signs mean that the hard photons precede the soft ones.

significant phase lag of -0.26 ± 0.08 rad. for the first overtone between the energy bands 2.8–8.7 and 8.7–60 keV. Although barely significant, this might indicate that also for the first overtone the hard photons preceded the soft ones.

Figure 6*g* shows that the noise component around 3–5 Hz in the first part of the data also had negative phase lags. The profile in phase lag diagram is rather narrow (narrower than the width of the noise component) and suggest that it might be due to a narrower noise component or even a QPO. To investigate this possibility, we examined the power spectra of the first part of the data in great detail for different energy ranges. We found that the noise component becomes more peaked at higher energies until it was nearly a true QPO (with a Q value of ~ 1.9 ; hereafter, we refer to this feature as QPO). In Figure 9, the power spectrum of the first part of the data is shown (only when all 5 PCUs were on) for the energy range 11.2–31.7 keV containing the QPO. Its strength was $9.8^{+0.8}_{-0.7}\%$ rms amplitude (6.7σ significance), its FWHM was $1.7^{+0.5}_{-0.3}$ Hz, and its frequency was 3.2 ± 0.1 Hz. Below 11.2 keV either this QPO was significantly broader or an extra noise component was present, which makes the QPO upper limits at lower energies difficult to obtain. A conservative upper limit can be given by assuming that all the power present is due to the QPO. This results in an upper limit of 4.5% and 1.1% for the energy ranges 4.3–11.2 keV and 2–4.3 keV, respectively. The QPO phase lag between 2.8–8.7 and 8.7–60 keV was -2.4 ± 0.2 radian, which absolute value is larger than the absolute value of the phase lag of the 5 Hz QPO (see Tab. 2). For both QPOs the hard photons precede the soft ones.

Recently, QPOs above 100 Hz were found in several BHC, simultaneously with QPOs round 5–7 Hz (e.g., Homan

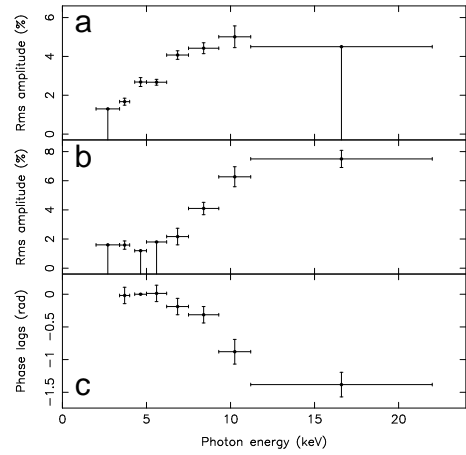


Figure 7. The rms amplitude of the fundamental (*a*), the rms amplitude of the overtone (*b*), and the phase lags of the fundamental (*c*) versus photon energy. In (*c*) the reference band chosen was 4.3–5.0 keV. Negative signs mean that the hard photons precede the soft ones.

et al. 2001; Cui et al. 2000). We searched the data for similar QPOs in GRS 1739–278, but none were found. The 95% confidence upper limits between 100 and 1000 Hz are 2.3% rms (1.7% rms) and 2.3% rms (1.8% rms), respectively for 2–60 keV and 4.3–60 keV, assuming a width of 150 Hz (the values for a FWHM of 50 Hz are given between brackets).

4 DISCUSSION

We present a detailed study of the 5 Hz QPO in the bright X-ray transient and black-hole candidate GRS 1739–278. This QPO was only observed during one *RXTE* observation (on 1996 March 31) during which the source was in state which can be identified as a very-high state (see also Borozdin et al. 1998). However, it is clear that the source was not at its highest possible luminosity demonstrating that very-high state behaviour can also occur at low luminosities, similar to what has been found in other BHCs (e.g., Homan et al. 2001). We showed that only during the second part of the observation the 5 Hz QPO and its first overtone were prominently present. During the first part only a broad noise component was present for energies below 10 keV and a broad QPO near 3 Hz for energies above that. All the QPOs considerably increased in strength with increasing photon energies, and the phase lags for all the QPOs demonstrate that the hard photons preceded the soft ones by as much as 1.5–2.5 radian.

The similarities between the 3 Hz QPO and the 5 Hz QPO (see Tab. 2) strongly suggests that they are directly related to each other. Most likely, the 3 Hz QPO evolved in the 5 Hz QPO, during which the frequency of the QPO increased, the energy dependence of the QPO became less dependent on energy, and the soft phase lag dropped from 2.5 radian to ~ 1 radian (between the energy ranges 2.8–8.7 keV and 8.7–60 keV). Unfortunately, this evolution occurred during an Earth occultation of the source and a passage of the satellite through the SAA, so a detail study of this process could not be made. From the X-ray colours and the

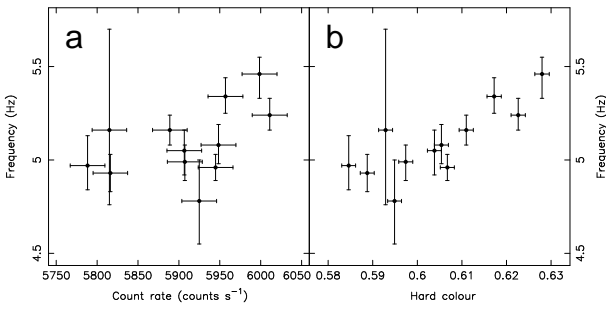


Figure 8. The frequency of the fundamental versus the 2–60 keV count rate (*a*) and the hard colour (*b*). The count rates were corrected for back-ground and collimator off-set, but not for dead-time. The hard colour is the 6.2–16.2 keV/2.2–3.7 keV count rate ratio.

HIDs and CD, it is clear that a small but significant spectral difference is present between the two parts of the observation, with the part containing the 5 Hz QPO slightly harder than the part with the 3 Hz QPO. This shows that a very slight change of the X-ray spectrum is accompanied by a significant change in the rapid X-ray variability. Whatever triggered this change, it only minorly effected the X-ray spectrum. This significant difference between the two parts of the observation also makes it clear that during the VHS of GRS 1739–278, the accretion processes involved are far from stable but they are very dynamic on a time scale of less than an hour.

The difference between the first part and second part of the observation was not reported by Borozdin & Trudolyubov (2000), most likely because they combined both parts together in their analysis without performing any time selections. The 5 Hz QPO parameters quoted by them are therefore contaminated by the inclusion of the first part of the data which does not contain this feature. Therefore, we report a significantly larger strength for the 5 Hz QPO and its first overtone than Borozdin & Trudolyubov (2000).

Recently, the phase lags of the low-frequency QPOs in BHC have received a considerable amount of attention in the literature. However, so far the phenomenology of these QPOs and their phase lags in particular are far from understood. The lags have now been studied for 1–20 Hz QPOs in GS 1124–683 (Takizawa et al. 1997), XTE J1550–564 (Wijnands, Homan, & van der Klis 1999; Cui et al. 2000; Remillard et al. 2001), GRS 1915+105 (Reig et al. 2000; Lin et al. 2000; Tomsick & Kaaret 2001), XTE J1859+226 (Cui et al. 2000), and GRS 1739–278 (this study). The phase lags show a large variety of behaviour. The different harmonics can have all the same sign for the lags (e.g., GS 1124–683; GRS 1739–278; although the sign can be both positive or negative) or can have different signs (the so-called ‘alternating phase lags’; e.g., XTE J1550–564; GRS 1915+105). The situation is made even more complex by the very complex evolution of the phase lags in several sources (e.g., XTE J1550–564; GRS 1915+105).

Several theoretical studies have tried to address the complicated phase lags behaviour of the low-frequency QPOs in BHCs (e.g., Nobili et al. 2000; Böttcher & Liang

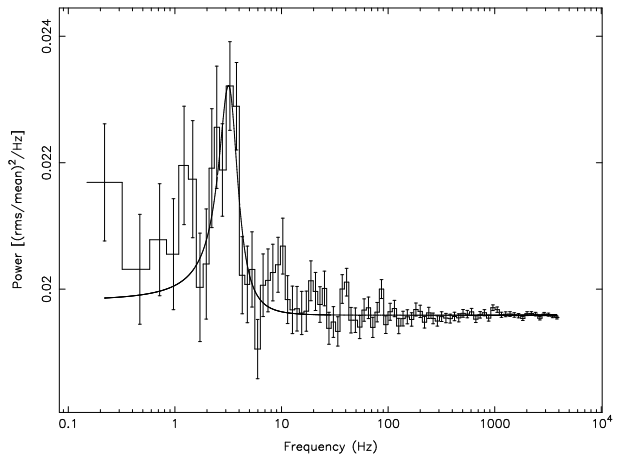


Figure 9. Power spectrum for the energy range 11.2–31.7 keV of the first data set (only the data for which all 5 PCUs were on) showing the 3 Hz QPO. The Poisson level has not been subtracted.

2000[‡]; Böttcher 2001), but those studies have focussed on the QPOs in GRS 1915+105. It is unclear to what extent the overall very complex behaviour of this source is influencing its QPO behaviour. Extrapolation from models for the behaviour (i.e., the QPOs and their phase lag behaviour) of GRS 1915+105 to other BHCs might turn out to be difficult and subject to errors. At the moment, there is no model available which can explain the observed phase lags of the QPOs, the evolution of those lags for the individual sources, and the differences between QPO behaviour in the different BHCs. However, it is clear that a Comptonizing medium around the black-hole (thought to produce the power-law tail in the spectrum) cannot explain the lags observed for the QPOs around 6 Hz, either due to Compton up- or down-scattering.

Recently, in several BHC transients QPOs above 100 Hz were found (e.g., Remillard et al. 1999a,b; Cui et al. 2000; Homan et al. 2001; Strohmayer 2001). Often, although not always, these QPOs are found simultaneously with low-frequency QPOs (<10 Hz), with similar characteristics as the 5 Hz QPO in GRS 1739–278. Therefore, similar high-frequency QPOs might also be present in GRS 1739–278. However, a search for such QPOs did not result in a significant detection, but the upper limits on the presence of such QPOs are not very stringent. Although in some sources stronger high-frequency QPOs have been found (e.g., XTE J1859+226; Cui et al. 2000), in other sources the high-frequency QPOs were considerable weaker than our upper limits (e.g., XTE J1550–564; Homan et al. 2001). Therefore, we cannot exclude that high frequency QPOs were present in GRS 1739–278.

[‡] Although submitted to ApJ for publication and available on astro-ph, this paper has been retracted for publication due to two major problems with the proposed QPO model: (1) the energy needed for the QPO mechanism to work exceeded that of the available energy, and (2) the predicted energy dependence of the QPO was the opposite to that observed (M. Böttcher 2001 private communication)

ACKNOWLEDGMENTS

This work was supported by NASA through Chandra Postdoctoral Fellowship grant number PF9-10010 awarded by CXC, which is operated by SAO for NASA under contract NAS8-39073. This research has made use of data obtained through the HEASARC Online Service, provided by the NASA/GSFC and quick-look results provided by the ASM/*RXTE* team.

REFERENCES

- Borozdin, K. N., & Trudolyubov, S. P. 2000, *ApJ*, 533, L131
- Borozdin, K., Alexandrovich, N., Sunyaev, R. 1996, *IAUC*, 6350
- Borozdin, K. N., Revnivtsev, M. G., Trudolyubov, S. P., Alexandrovich, N. L., Sunyaev, R. A., Skinner, G. K. 1998, *Astronomy Letters*, 24, 435 (astro-ph/9901192)
- Böttcher, M. 2001, *ApJ*, 553, 960
- Böttcher, M. & Liang, E. P. 2000, *ApJ*, submitted but retracted (astro-ph/0003139)
- Cui, W., Shrader, C. R., Haswell, C. A., Hynes, R. I. 2000, *ApJ*, 535, L123
- Dennerl, K., & Greiner, J. 1996, *IAUC*, 6426
- Dieters, S. W., Belloni, T., Kuulkers, E., Woods, P., Cui, W., Zhang, S. N., Chen, W., van der Klis, M., van Paradijs, J., Swank, J., Lewin, W. H. G., Kouveliotou, C. 2000, *ApJ*, 538, 307
- Greiner, J., Dennerl, K., Predehl, P. 1996, *A&A*, 314, L21
- Homan, J., Wijnands, R., van der Klis, M., Belloni, T., van Paradijs, J., Klein-Wolt, M., Fender, R., Méndez, M. 2001, *ApJS* 132, 377
- Hjellming, R. M., Rupen, M. P., Marti, J., Mirabel, F., Rodriguez, L. F. 1996, *IAUC*, 6384
- Leahy, D. A., Darbo, W., Elsner, R. F., Weisskopf, M. C., Kahn, S., Sutherland, P. G., Grindlay, J. E. 1983, *ApJ*, 266, 160
- Levine, A. M., Bradt, H., Cui, W., Jernigan, J. G., Morgan, E. H., Remillard, R., Shirey, R. E., Smith, D. A. 1996, *ApJ* 469, L33
- Lin, D., Smith, I. A., Liang, E. P., Böttcher, M. 2000, *ApJ*, 543, L141
- Marti, J., Mirabel, I. F., Duc, P.-A., Rodríguez, L. F. 1997, *A&A*, 323, 158
- Mirabel, I. F., Marti, J., Duc, P.-A., Rodríguez, L. F. 1996, *IAUC*, 6428
- Nobili, L., Turolla, R., Zampieri, L., Belloni, T. 2000, *ApJ*, 538, L137
- Paul, J., Bouchet, L., Churazov, E., Sunyaev, R. 1996, *IAUC*, 6348
- Psaltis, D., Belloni, T., van der Klis, M. 1999, *ApJ*, 520, 262
- Remillard, R. A., McClintock, J. E., Sobczak, G. J., Bailyn, C. D., Orosz, J. A., Morgan, E. H., & Levine, A. M. 1999a, *ApJ*, 517, L127
- Remillard, R. A., Morgan, E. H., McClintock, J. E., Bailyn, C. D., Orosz, J. A. 1999b, *ApJ*, 522, 397
- Remillard, R. A., Sobczak, G. J., Muno, M. P., McClintock, J. E. 2001, *ApJ* submitted (astro-ph/0105508)
- Reig, P., Belloni, T., van der Klis, M., Méndez, M., Kylafis, N. D., Ford, E. C. 2000, *ApJ*, 541, 883
- Revnivtsev, M. G., Trudolyubov, S. P., & Borozdin, K. N. 2000, *MNRAS*, 312, 151
- Strohmayer, T. 2001, *ApJ*, 552, L49
- Takeshima, T., Cannizzo, J. K., Corbet, R., Marshall, F. E. 1996, *IAUC*, 6390
- Takizawa, M., et al. 1997, *ApJ*, 489, 272
- Tanaka, Y., & Lewin, W. H. G. 1995, In: *X-ray Binaries*, W. H. G. Lewin, J. van Paradijs, & E. P. J. van den Heuvel (eds.), Cambridge University Press, p. 126

- Tomsick, J. A. & Kaaret, P. 2001, *ApJ*, 548, 401
- van der Klis, M. 1995, In: *X-ray Binaries*, W. H. G. Lewin, J. van Paradijs, & E. P. J. van den Heuvel (eds.), Cambridge University Press, p. 252
- van der Klis, M., Hasinger, G., Stella, L., Langmeier, A., van Paradijs, J., & Lewin, W. H. G. 1987, *ApJ*, 319, 113
- Vargas M., et al. 1997, *ApJ*, 476, L23
- Wijnands, R., Homan, J., van der Klis, M. 1999, *ApJ*, 526, L33

Table 1. QPO parameters versus photon energy^a

Photon energy range (keV)	Fundamental amplitude (% rms)	Overtone amplitude (% rms)	Fundamental phase lag ^b (rad)
2–3.4	<1.3	<1.6	–
3.4–4.0	1.67±0.18	1.59±0.29	–0.003±0.02
4.3–5.0	2.68±0.23	<1.2	0 ^c
5.0–6.2	2.67±0.15	<1.8	0.002±0.02
6.2–7.5	4.07±0.22	2.17±0.57	–0.03±0.02
7.5–9.3	4.42±0.28	4.10±0.43	–0.05±0.02
9.3–11.2	5.01±0.56	6.27±0.69	–0.14±0.03
11.2–22.0	<4.5	7.50±0.59	–0.22±0.03
3.4–5.6	2.10±0.08	1.32±0.18	–
5.6–7.5	3.62±0.14	1.84±0.36	–

^a The errors on the fit parameters are for $\Delta\chi^2 = 1.0$ and the upper limits are for 95% confidence levels

^b Calculated for the 1.11 Hz interval (the FWHM of the QPO) centred on the peak frequency of the QPO (5.09 Hz)

^c Reference band

Table 2. The 3 Hz QPO vs. the 5 Hz QPO

Frequency (Hz)	Amplitude			Phase lags ^a (radian)
	2–4.3 keV (% rms)	4.3–11.2 keV (% rms)	11.2–31.7 keV (% rms)	
3.2±0.1	<1.1	<4.5	9.8 ^{+0.8} _{–0.7}	–2.4±0.2
5.09±0.02	1.3±0.1	3.15±0.07	<4.5	–1.01±0.06

^a Between the energy bands 2.8–8.7 keV and 8.7–60 keV